



THE UNIVERSITY *of* EDINBURGH

Edinburgh Research Explorer

Connecting atmospheric blocking to European temperature extremes in spring

Citation for published version:

Brunner, L, Hegerl, GC & Steiner, AK 2017, 'Connecting atmospheric blocking to European temperature extremes in spring', *Journal of Climate*. <https://doi.org/10.1175/JCLI-D-16-0518.1>

Digital Object Identifier (DOI):

[10.1175/JCLI-D-16-0518.1](https://doi.org/10.1175/JCLI-D-16-0518.1)

Link:

[Link to publication record in Edinburgh Research Explorer](#)

Document Version:

Peer reviewed version

Published In:

Journal of Climate

Publisher Rights Statement:

© 2016 American Meteorological Society

General rights

Copyright for the publications made accessible via the Edinburgh Research Explorer is retained by the author(s) and / or other copyright owners and it is a condition of accessing these publications that users recognise and abide by the legal requirements associated with these rights.

Take down policy

The University of Edinburgh has made every reasonable effort to ensure that Edinburgh Research Explorer content complies with UK legislation. If you believe that the public display of this file breaches copyright please contact openaccess@ed.ac.uk providing details, and we will remove access to the work immediately and investigate your claim.





AMERICAN METEOROLOGICAL SOCIETY

Journal of Climate

EARLY ONLINE RELEASE

This is a preliminary PDF of the author-produced manuscript that has been peer-reviewed and accepted for publication. Since it is being posted so soon after acceptance, it has not yet been copyedited, formatted, or processed by AMS Publications. This preliminary version of the manuscript may be downloaded, distributed, and cited, but please be aware that there will be visual differences and possibly some content differences between this version and the final published version.

The DOI for this manuscript is doi: 10.1175/JCLI-D-16-0518.1

The final published version of this manuscript will replace the preliminary version at the above DOI once it is available.

If you would like to cite this EOR in a separate work, please use the following full citation:

Brunner, L., G. Hegerl, and A. Steiner, 2016: Connecting atmospheric blocking to European temperature extremes in spring. *J. Climate*. doi:10.1175/JCLI-D-16-0518.1, in press.



Connecting atmospheric blocking to European temperature extremes in spring

Lukas Brunner*

*Wegener Center for Climate and Global Change (WEGC),
 Institute for Geophysics, Astrophysics, and Meteorology/Institute of Physics,
 and FWF-DK Climate Change, University of Graz, Graz, Austria*

Gabriele C. Hegerl

School of Geosciences, University of Edinburgh, Edinburgh, UK

Andrea K. Steiner

*Wegener Center for Climate and Global Change (WEGC),
 Institute for Geophysics, Astrophysics, and Meteorology/Institute of Physics,
 and FWF-DK Climate Change, University of Graz, Graz, Austria*

* Corresponding author address: Lukas Brunner, Wegener Center for Climate and Global Change,

Brandhofgasse 5, 8010-Graz, Austria.

E-mail: lukas.brunner@uni-graz.at

ABSTRACT

16 Atmospheric blocking is an important contributor to European temperature
17 variability. It can trigger cold and warm spells, which is of specific relevance
18 in spring because vegetation is particularly vulnerable to extreme tempera-
19 tures in the growing season. The spring season is investigated as transition
20 period from predominant connections of blocking with cold spells in winter
21 to predominant connections of blocking with warm spells in summer. Ex-
22 treme temperatures are termed cold or warm spells if temperature stays out-
23 side the 10th to 90th percentile range for at least 6 consecutive days. Cold
24 and warm spells in Europe over 1979 to 2014 are analyzed in observations
25 from E-Obs data and the connection to blocking is examined in geopotential
26 height fields from ERA-Interim. A highly significant link between blocking
27 and cold and warm spells is found which changes during spring. Blocking
28 over the north-eastern Atlantic and Scandinavia is correlated with the occur-
29 rence of cold spells in Europe, particularly early in spring, while blocking
30 over central Europe is associated with warmer conditions, particularly from
31 March onwards. The location of the block also impacts the spatial distribu-
32 tion of temperature extremes. More than 80 % of cold spells in south-eastern
33 Europe occur during blocking whereas warm spells are correlated to blocking
34 mainly in northern Europe. Over the analysis period, substantial interannual
35 variability is found but also a decrease in cold spells and an increase in warm
36 spells. The long-term change to a warmer climate holds the potential for even
37 higher vulnerability to spring cold extremes.

38 **1. Introduction**

39 European weather and climate is strongly influenced by large-scale circulation patterns such
40 as the Atlantic storm tracks, the jet stream, and atmospheric blocking (e.g., Woollings 2010).
41 Atmospheric blocking describes a meteorological situation in which a persistent and stationary
42 high pressure system blocks the climatological westerly flow at mid-latitudes for several days to
43 weeks (Rex 1950; Tibaldi and Molteni 1990; Pelly and Hoskins 2003; Barriopedro et al. 2006;
44 Croci-Maspoli et al. 2007).

45 Extremes on both ends of the temperature distribution are especially closely connected to atmo-
46 spheric blocking. Increased cold spell frequency is found during blocked conditions in European
47 winter (Buehler et al. 2011) and up to 80 % of summer hot temperature extremes in northern Eu-
48 rope are associated with a co-located blocking (Pfahl and Wernli 2012). Atmospheric blocking
49 has also been identified as main contributor to specific extreme events such as the cold European
50 winter in 2010 (Cattiaux et al. 2010) or the Russian heatwave in summer 2010 (Matsueda 2011).

51 Surface temperatures can be impacted by atmospheric blocking via radiative forcing or advec-
52 tion. Radiative effects are mainly constrained to the center of the block where clear-sky conditions
53 favor positive temperature anomalies. The anticyclonic circulation of the block affects tempera-
54 tures especially on the eastern and southern flanks by advection of cold air from the north and east
55 (e.g., Trigo et al. 2004; Bieli et al. 2015). A range of studies has either focused on the predominant
56 cooling effect of blocking in winter (Trigo et al. 2004; Barriopedro et al. 2008; Cattiaux et al.
57 2010; Buehler et al. 2011; Sillmann et al. 2011; Whan et al. 2016) or on the warming effect in
58 summer (Xoplaki et al. 2003; Cassou et al. 2005; Pfahl and Wernli 2012; Stefanon et al. 2012).
59 Recently, Cassou and Cattiaux (2016) showed that the transition between blocking being linked

60 to anomalously cold conditions in winter to blocking being linked to warm conditions in summer
61 has shifted by a few days due to climate warming.

62 Here we investigate the link between atmospheric blocking and European cold and warm spells
63 during spring to provide better insight into the shifting role of blocking for extremes during this
64 transition period. Spring temperature extremes are of special relevance because vegetation during
65 this season is particularly vulnerable to abnormal temperatures. Late spring frost can severely
66 harm or even destroy fresh leaves, subsequently requiring considerable additional resource use
67 by plants. Correspondingly, warm spells in early spring can lead to premature greening onset
68 (Hufkens et al. 2012; Menzel et al. 2015, and references therein). Ma et al. (2016) showed the
69 potential of earlier spring green-up to also impact European warm spells via feedback processes.
70 In this study we analyze the connection of blocking and extreme temperature occurrences, their
71 spatial distribution and change over the last decades. We focus on spring on a month-by-month
72 basis, but also show results for the seasonal mean of other seasons. We describe data and methods
73 in section 2. Results are presented in section 3 and a summary is given in section 4.

74 **2. Data and Methods**

75 The detection of temperature extremes is based on E-Obs version 12.0 (Haylock et al. 2008),
76 an observational, land-only data set for Europe. It comprises measurements from a network of
77 more than 2000 irregularly distributed meteorological stations interpolated to a regular grid (Klok
78 and Klein Tank 2009). In this study we investigate daily minimum temperature (T_{\min}) and daily
79 maximum temperature (T_{\max}) on a $0.25^\circ \times 0.25^\circ$ longitude-latitude grid between 1979 and 2014.
80 We detect cold and warm spells in mainland Europe and the British Isles (12.5°W to 30°E and
81 35°N to 72.5°N). First, the daily linear trend from 1979 to 2014 is subtracted from each grid point
82 in the E-Obs temperatures to remove the long-term temperature trend. Daily 10th/90th percentiles

83 of T_{\min}/T_{\max} are computed over the 36 year period using a 21 day sliding window. A grid point
84 with T_{\min} below the 10th percentile or T_{\max} above the 90th percentile for at least 6 consecutive
85 days is identified as cold or warm extreme, respectively. This study focuses on large scale events
86 on a daily basis. Therefore we define a cold spell day (CSD) or warm spell day (WSD) if at least
87 400 grid points (i.e., $5^\circ \times 5^\circ$) simultaneously are found to be exposed to a cold or warm extreme
88 criterion on a given day. Resulting cold/warm spells are found to be spatially highly coherent, so
89 no separate adjacence-criterion was applied.

90 The detection of blocking is based on daily geopotential height (GPH) fields from the European
91 Centre for Medium-Range Weather Forecasts (ECMWF) re-analysis Interim (ERA-Interim) (Dee
92 et al. 2011) at a $2.5^\circ \times 2.5^\circ$ longitude-latitude grid, which is available from 1979 onward. We
93 apply a standard algorithm utilizing the reversal of mid-latitude 500 hPa GPH gradients (Tibaldi
94 and Molteni 1990; Scherrer et al. 2006; Davini et al. 2012, 2014), detailed in Brunner et al. (2016).
95 The blocking detection algorithm identifies high pressure systems associated with an overturning
96 of the flow and selects extended and persistent events of at least 5 days duration. Therefore this
97 classical approach covers stationary and isolated high pressure systems northward of 45°N . We
98 compute blocking frequencies on a grid point basis for climatological conditions as well as for
99 CSDs and WSDs. We subsequently define a blocked day if blocking is found anywhere in the
100 Euro-Atlantic blocking region (30°W to 45°E and 45°N to 72.5°N) (Barriopedro et al. 2010; IPCC
101 2013) on a certain day. We then also investigate the relative frequency of CSDs and WSDs on a
102 grid point basis during blocked and unblocked days. This approach allows to simultaneously
103 investigate the local and remote effects of blocking on CSDs and WSDs.

104 In addition, we analyse selected subdomains and investigate the importance of the location of
105 cold/warm spells and blocking for their connection. For selection for CSDs/WSDs in subdomains
106 we adjust the spatial criterion to consider CSDs/WSDs with more than half of their grid points in

107 the selected subdomain. For selection of blocking in subdomains we consider blocks with at least
108 one blocked grid point in the selected subdomain.

109 In order to test any co-occurrence of CSDs/WSDs and blocked days for significance we perform
110 a Monte-Carlo test. Given N CSDs/WSDs in a period (i.e., month or season), we draw 1000 ran-
111 dom samples of N days from the same period. To ensure that each random sample yields the same
112 auto-correlation at all lags the samples are drawn as clusters of days similar as represented in the
113 original data set. We then calculate for each random sample of N days the blocking frequency on
114 a grid point basis as well as the occurrence of blocked days in the blocking region. The correlation
115 between blocking and CSDs/WSDs is considered statistically significant if the blocking frequency
116 during CSDs/WSDs on a grid point or if the number of blocked CSDs/WSDs is smaller than the
117 5th or larger than the 95th percentile of the joined probability density function (PDF) established
118 over all 1000 random samples, respectively. The same considerations are made for the statistical
119 significance of CSDs/WSDs given the number of blocked days in each period.

120 **3. Results**

121 The time evolution of blocked and extreme days over time is presented in Fig. 1. Over the
122 spring season (MAM), a decrease in the number of CSDs (both, generally and if restricted to
123 blocked days) is found towards late spring (Fig. 1a, right). Over 1979 to 2014, the seasonal mean
124 time series (Fig. 1c, top) show periods with less or more CSDs, pointing at significant interannual
125 variability. A considerable number of CSDs exhibits blocking several days before their onset,
126 indicating that a certain amount of time is necessary to lower the temperature sufficiently for a
127 cold spell to develop (Fig. 1a, main panel), consistent with findings of Buehler et al. (2011). If
128 the trend in the underlying temperature time series is not removed (Fig. 1c, bottom) we find more
129 CSDs at the beginning of the period and a lack of CSDs at the end of the period, indicating that

130 extended cold periods are restrained to winter in a warming climate. However, some lack of cold
131 spells also occurs after de-trending (Fig. 1c, top), pointing at the role of internal variability.

132 Over the spring season, the number of WSDs and with it the number of blocked WSDs increases
133 towards summer (Fig. 1b, right). Over the analysis period, the seasonal mean time series also show
134 considerable interannual variability for WSDs (Fig. 1d, top). If the trend is not removed from the
135 underlying temperature time series (Fig. 1d, bottom) an increase of the number of WSDs (both,
136 generally and if restricted to blocked conditions) in the investigated period from 1979 to 2014 is
137 evident, consistent with the detection of changes in the number of temperature extremes in Europe
138 (Zwiers et al. 2011; IPCC 2013; Morak et al. 2013). Note that all subsequent discussions refer
139 exclusively to the de-trended data.

140 A complete summary of statistics for CSDs/WSDs in spring and all individual months of the
141 extended spring season (February to June) is shown in Table 1. We also included results for the
142 summer (JJA), fall (SON), and winter (DJF) seasons for comparison. Our results generally indi-
143 cate that blocking plays a strong role in spring/summer warm spells and in fall/winter cold spells,
144 consistent with the literature (e.g., Cassou and Cattiaux 2016). In total about 46 % of CSDs in
145 spring are blocked days and about 10 % of blocked spring days coincide with a CSD. A statis-
146 tically significant link is found in the extended spring season in February (correlation) and June
147 (anti-correlation) as well as in winter (correlation) and in summer (anti-correlation; cf. Table 1).
148 Regarding WSDs in spring, a statistically significant fraction of 54 % is blocked and about 21 %
149 blocked spring days coincide with a WSD. Also most individual months of the extended spring
150 show a significant correlation with blocking (as do summer months), except February on the transi-
151 tion from winter to spring exhibits a significant anti-correlation (as do winter months; cf. Table 1).

152 Analyzing blocking on a grid point basis, the climatological blocking frequency in the Euro-
153 Atlantic region is generally between 2 % and 6 % of spring days. The blocking frequency coin-

ciding with CSDs in spring is depicted in Fig. 2a. Three distinct regions are revealed: west of the British Isles (i) and over northern Scandinavia (ii) the blocking frequency is up to three times higher for CSDs than for climatological conditions and differs statistically significantly from the random sample. This is consistent with cold advection during such blocks into central and western Europe. Over central and eastern Europe (iii) there is significantly less blocking during CSDs ($<2\%$) than in the climatology since blocking occurring there tends to lead to warmer, fair weather conditions.

A closer investigation of the extended spring season based on monthly frequencies reveals how the role of blocking associated with CSDs changes through spring (Fig. 2b-f). February and March show significantly increased blocking frequency northward of 60°N (exceeding 16% and 12% , respectively), indicating a strong link of blocking in this region to cold conditions in Europe in late winter/early spring. Between March and April a distinct change is obvious where maximum blocking frequencies shift from northern Europe to the west of the British Isles. This change may be founded in the temperature seasonality over the European continent: in winter the continent is still relatively cold, such that easterly flow is sufficient to lead to CSDs, while northerly advection with blocking to the west is necessary as the continent warms up in later spring. The CSD blocking frequency in central and eastern Europe is lowered during all spring months highlighting the anti-correlation between cold conditions and blocking in this region. In June where only about 3% of total days are associated with a cold spell (cf. Table 1) no significant relationship with blocking is found.

The blocking frequency coinciding with WSDs in spring is found to be up to three times higher than during climatological conditions (Fig. 3a) and statistically significantly different from the random sample in most of Europe. Blocks linked to warm spells are distributed across Europe, while there are less than average blocking days associated with WSDs west of the British Isles.

178 The anti-cyclonic motion of blocking highs in the latter area would favor cold advection into
179 Europe, consistent with the results for CSDs (Fig. 2).

180 Resolving individual months (Fig. 3b-f) reveals that in February the link between blocking
181 and WSDs is mostly negative. Over the entire winter season, a significant and widespread anti-
182 correlation is found between warm spells and blocking in the west and north of the Euro-Atlantic
183 blocking region (not shown). However, over central Europe increased blocking frequencies on
184 WSDs can be found in February and in winter, indicating that fair-weather conditions connected
185 with blocking highs can lead to winter warm spells here. From March onward the WSD blocking
186 frequency shows a strong increase and is significantly higher than the climatological mean. The
187 maximum of the frequency shifts slightly to the north towards summer.

188 Having analyzed the distribution of blocking frequencies, we now reversely investigate the spa-
189 tial distribution of grid points contributing to CSDs/WSDs (termed CSDs/WSDs per grid point)
190 in the European region. Fig. 4a, b show the number of CSDs and WSDs per grid point over 36
191 springs from 1979 to 2014, respectively. The fraction of CSDs and WSDs per grid point during
192 1363 blocked days in spring (Fig. 4c, d) reveals a distinct dipole pattern for both cases. While in
193 total about 46 % of CSDs are blocked in spring (cf. Table 1), in south-eastern Europe more than
194 80 % of CSDs per grid point are blocked. In contrast, a strong anti-correlation is found over the
195 British Isles and in Scandinavia, where less than 30 % of CSDs per grid point coincide with block-
196 ing. For WSDs per grid point the opposite picture arises with locally more than 80 % associated
197 with blocking northward of 50°N. In south-eastern Europe statistically significant anti-correlation
198 is found with less than 40 % of WSDs per grid point connected to blocking. This is consistent
199 with the preferential location of blocks during WSDs which is largely limited to Northern Eu-
200 rope (Fig. 3), particularly later in spring. Differences of T_{\min}/T_{\max} composites of blocked minus
201 unblocked CSDs/WSDs show a similar dipole pattern: both, CSDs and WSDs, with a blocking

anywhere in the blocking region are warmer in Scandinavia and colder in mainland Europe than without a blocking.

For a closer investigation of the dipole feature we divide Europe into two subdomains for CSDs/WSDs: northern ($> 50^{\circ}\text{N}$) and southern ($< 50^{\circ}\text{N}$) Europe (cf. Fig. 4c, d). Selecting only CSDs/WSDs in these subdomains we show the corresponding blocking frequency in Fig. 5. For the 163 CSDs in northern Europe hardly any blocking is found in the entire Euro-Atlantic blocking region (Fig. 5a) indicating that blocking tends to counteract CSDs here. CSDs (136 days) in southern Europe (Fig. 5c) are clearly linked to the blocking regions west of the British Isles and over Scandinavia indicated by distinct maximum blocking frequencies exceeding 18 %. Considering in reverse only blocking west of the British Isles (cf. Fig. 2a) we consistently find correlation predominantly with CSDs in south-eastern Europe. Considering only blocking in northern Scandinavia (cf. Fig. 2a) leads to statistically significantly increased CSDs per grid point in most of central and eastern Europe (not shown).

WSDs in northern Europe (247 days) are found clearly connected to blocking over Scandinavia with highest blocking frequencies exceeding 20 % (Fig. 5b). Consistently blocking over Scandinavia is correlated with increased frequency of WSDs in most of northern Europe in spring. In contrast, WSDs in southern Europe are connected to reduced blocking frequencies northward of 60°N (Fig. 5d). These results show the importance of the location of blocking and are consistent with a strong role of cold advection at the edges of blocks for CSDs and increased solar radiation leading to WSDs in blocked regions.

4. Summary and discussion

We analyzed the relationship between blocking occurrence and temperature extremes in European spring for the period 1979 to 2014. Our results show statistically significant correlations of

225 blocking frequency and the occurrence of cold spells and warm spells throughout the spring sea-
226 son, with sensitivity to the location of the block. We found blocking in winter and early spring
227 to be stronger connected to cold conditions while blocking in late spring and summer is stronger
228 connected to warm conditions. Blocked days in February show a statistically significant correla-
229 tion with cold spell days whereas blocking in April is statistically significantly correlated to warm
230 spell days, suggesting that on average the blocking-temperature relationship changes sign during
231 this time.

232 Over the spring season, the number of cold spell days decreases towards late spring whereas
233 the number of warm spell days increases. Over the analysis period, the seasonal mean time se-
234 ries show considerable interannual variability for both, cold and warm spells. If the trend is not
235 removed from the underlying temperature time series, a lack of cold spell days and a clustering
236 of warm spell days in late spring in the last 15 years of the investigated period suggest that the
237 underlying long-term global warming trend also influences the frequency of cold spell days and
238 warm spell days. In contrast, there is no apparent trend in the number of blocked days, suggest-
239 ing that the trend is due to large scale warming rather than a change in circulation. The shift in
240 probability of less cold extremes towards a higher probability of warm extremes, particularly in
241 late spring, is consistent with recent findings on the earlier onset of summer and disruption of the
242 European seasonal clock (Cassou and Cattiaux 2016). In such a warmer climate the occurrence of
243 a cold spell in spring becomes even more critical and detrimental to vegetation as just recently hap-
244 pened in Europe. After exceptionally warm spring temperatures, central and south-eastern Europe
245 were affected by a cold spell in late April 2016 which caused large damages on crops, orchards
246 and vineyards especially in Austria, Slovenia, Slovakia, and Croatia (AGRI4CAST 2016). Our
247 findings lay the basis for further research into these changes, the atmospheric dynamics driving

248 the relationship of blocking and temperature extremes, and potential contributions to improved
249 seasonal forecasting.

250 The location of the block is found also essential for its impact on European extreme tempera-
251 tures. Blocking west of the British Isles and over northern Scandinavia is clearly connected with
252 cold spells in southern Europe while blocking over central Europe and southern Scandinavia is
253 associated with warm spells in northern Europe. This is consistent with the role of cold advec-
254 tion at the edges of blocks leading to cold spells outside blocked regions and with increased solar
255 radiation leading to warm spells in blocked regions.

256 The spatial distribution of cold and warm spells during blocking reveals a distinct dipole pattern.
257 Cold spells in south-eastern Europe are found highly correlated with blocking, and more than 80 %
258 of cold spell days co-occur with a blocking. In contrast, cold spells in northern Scandinavia and
259 blocking are anti-correlated with regionally less than 30 % co-occurrence. Warm spells show
260 the opposite relationship with locally more than 80 % of warm spell days in northern Europe co-
261 occurring with blocking, but anti-correlation in southern Europe. An increased occurrence of both,
262 warm and cold spells during blocked conditions is found around 50°N indicating that blocking
263 increases the probability for both high and low temperature extremes here.

264 The occurrence of atmospheric blocking in the European region is found to be crucial for the
265 development of both, extended cold and warm spells, in spring. We provide insight into the chang-
266 ing role of blocking in spring as its connection to cold conditions decreases and the connection to
267 warm conditions increases. Our findings furthermore underline the importance of the location of
268 blocking for its correlation with either cold or warm spells, highlighting in particular the remote
269 effects of blocking on European temperatures.

270 *Acknowledgments.* The authors thank T. Woollings (University of Reading, UK) and participants
271 of the 2016 SPARC workshop on atmospheric blocking (Reading, UK) for fruitful discussions
272 and helpful comments, and S. Morak (University of Edinburgh, UK) for results from earlier work.
273 We acknowledge the E-OBS dataset from the EU-FP6 project ENSEMBLES ([http://ensembles-](http://ensembles-eu.metoffice.com)
274 [eu.metoffice.com](http://ensembles-eu.metoffice.com)) and the data providers in the ECA&D project (<http://www.ecad.eu>). ECMWF
275 (Reading, UK) is acknowledged for access to its ERA-Interim data set. This work was funded
276 by the Austrian Science Fund (FWF) under research grant W 1256-G15 (Doctoral Programme
277 Climate Change – Uncertainties, Thresholds and Coping Strategies). G. Hegerl was supported by
278 the ERC funded project TITAN (EC-320691), by the Wolfson Foundation and the Royal Society
279 as a Royal Society Wolfson Research Merit Award (WM130060) holder, by the EUCLEIA project
280 funded by the European Union’s Seventh Framework Programme (FP7/2007-2013) under Grant
281 Agreement No. 607085, and by NCAS.

282

283 The authors thank the editor D. Waugh and three anonymous reviewers for their helpful com-
284 ments on the manuscript.

285 **References**

286 AGRI4CAST, 2016: JRC MARS Bulletin – Crop monitoring in Europe. European
287 Commission/Joined Research Centre, URL [https://ec.europa.eu/jrc/sites/default/files/](https://ec.europa.eu/jrc/sites/default/files/jrc-mars-bulletin-vol24-no5.pdf)
288 [jrc-mars-bulletin-vol24-no5.pdf](https://ec.europa.eu/jrc/sites/default/files/jrc-mars-bulletin-vol24-no5.pdf).

289 Barriopedro, D., R. García-Herrera, and R. Huth, 2008: Solar modulation of Northern Hemisphere
290 winter blocking. *J. Geophys. Res.*, **113** (D14), D14118, doi:10.1029/2008JD009789.

291 Barriopedro, D., R. García-Herrera, A. R. Lupo, and E. Hernández, 2006: A climatology of north-
 292 ern hemisphere blocking. *J. Climate*, **19**, 1042–1063, doi:10.1175/JCLI3678.1.

293 Barriopedro, D., R. García-Herrera, and R. M. Trigo, 2010: Application of blocking diagnosis
 294 methods to General Circulation Models. Part I: a novel detection scheme. *Climate Dyn.*, **35** (7–
 295 **8**), 1373–1391, doi:10.1007/s00382-010-0767-5.

296 Bieli, M., S. Pfahl, and H. Wernli, 2015: A Lagrangian investigation of hot and cold temperature
 297 extremes in Europe. *Quart. J. Roy. Meteor. Soc.*, **141** (**686**), 98–108, doi:10.1002/qj.2339.

298 Brunner, L., A. K. Steiner, B. Scherllin-Pirscher, and M. W. Jury, 2016: Exploring atmospheric
 299 blocking with GPS radio occultation observations. *Atmos. Chem. Phys.*, **16** (**7**), 4593–4604,
 300 doi:10.5194/acp-16-4593-2016.

301 Buehler, T., C. C. Raible, and T. F. Stocker, 2011: The relationship of winter season North Atlantic
 302 blocking frequencies to extreme cold or dry spells in the ERA-40. *Tellus A*, **63** (**2**), 212–222,
 303 doi:10.1111/j.1600-0870.2010.00492.x.

304 Cassou, C., and J. Cattiaux, 2016: Disruption of the European climate seasonal clock in a warming
 305 world. *Nature Climate Change*, **6**, 589–594, doi:10.1038/nclimate2969.

306 Cassou, C., L. Terray, and A. S. Phillips, 2005: Tropical Atlantic influence on European heat
 307 waves. *J. Climate*, **18**, 2805–2811, doi:10.1175/JCLI3506.1.

308 Cattiaux, J., R. Vautard, C. Cassou, P. Yiou, V. Masson-Delmotte, and F. Codron, 2010: Winter
 309 2010 in Europe: A cold extreme in a warming climate. *Geophys. Res. Lett.*, **37** (**20**), L20704,
 310 doi:10.1029/2010GL044613.

311 Croci-Maspoli, M., C. Schwierz, and H. C. Davies, 2007: A multifaceted climatology of atmo-
 312 spheric blocking and its recent linear trend. *J. Climate*, **20** (4), 633–649, doi:10.1175/JCLI4029.
 313 1.

314 Davini, P., C. Cagnazzo, P. G. Fogli, E. Manzini, S. Gualdi, and A. Navarra, 2014: European
 315 blocking and Atlantic jet stream variability in the NCEP/NCAR reanalysis and the CMCC-CMS
 316 climate model. *Climate Dyn.*, **43** (1–2), 71–85, doi:10.1007/s00382-013-1873-y.

317 Davini, P., C. Cagnazzo, S. Gualdi, and A. Navarra, 2012: Bidimensional diagnostics, variabil-
 318 ity, and trends of Northern Hemisphere blocking. *J. Climate*, **25**, 6496–6509, doi:10.1175/
 319 JCLI-D-12-00032.1.

320 Dee, D. P., and Coauthors, 2011: The ERA-Interim reanalysis: configuration and performance of
 321 the data assimilation system. *Quart. J. Roy. Meteor. Soc.*, **137** (656), 553–597, doi:10.1002/qj.
 322 828.

323 Haylock, M. R., N. Hofstra, A. M. G. Klein Tank, E. J. Klok, P. D. Jones, and M. New, 2008:
 324 A European daily high-resolution gridded data set of surface temperature and precipitation for
 325 1950–2006. *J. Geophys. Res.*, **113** (D20), D20119, doi:10.1029/2008JD010201.

326 Hufkens, K., M. A. Friedl, T. F. Keenan, O. Sonnentag, A. Bailey, J. O’Keefe, and A. D. Richard-
 327 son, 2012: Ecological impacts of a widespread frost event following early spring leaf-out. *Glob.*
 328 *Change Biol.*, **18** (7), 2365–2377, doi:10.1111/j.1365-2486.2012.02712.x.

329 IPCC, 2013: *Climate Change 2013: The Physical Science Basis. Contribution of Working Group I*
 330 *to the Fifth Assessment Report of the Intergovernmental Panel on Climate Change*. Cambridge
 331 University Press, Cambridge, United Kingdom and New York, NY, USA, 1535 pp.

332 Klok, E. J., and A. M. G. Klein Tank, 2009: Updated and extended European dataset of daily
 333 climate observations. *Int. J. Climatol.*, **29** (8), 1182–1191, doi:10.1002/joc.1779.

334 Ma, S., A. J. Pitman, R. Lorenz, J. Kala, and J. Srbinovsky, 2016: Earlier green-up and
 335 spring warming amplification over Europe. *Geophys. Res. Lett.*, **43** (5), 2011–2018, doi:
 336 10.1002/2016GL068062.

337 Matsueda, M., 2011: Predictability of Euro-Russian blocking in summer of 2010. *Geophys. Res.*
 338 *Lett.*, **38** (6), L06801, doi:10.1029/2010GL046557.

339 Menzel, A., R. Helm, and C. Zang, 2015: Patterns of late spring frost leaf damage and recovery in
 340 a European beech (*Fagus sylvatica* L.) stand in south-eastern Germany based on repeated digital
 341 photographs. *Frontiers in Plant Science*, **6** (110), doi:10.3389/fpls.2015.00110.

342 Morak, S., G. C. Hegerl, and N. Christidis, 2013: Detectable changes in the frequency of temper-
 343 ature extremes. *J. Climate*, **26** (5), 1561–1574, doi:10.1175/JCLI-D-11-00678.1.

344 Pelly, J. L., and B. J. Hoskins, 2003: A new perspective on blocking. *J. Atmos. Sci.*, **60**, 743–755,
 345 doi:10.1175/1520-0469(2003)060<0743:ANPOB>2.0.CO;2.

346 Pfahl, S., and H. Wernli, 2012: Quantifying the relevance of atmospheric blocking for co-located
 347 temperature extremes in the Northern Hemisphere on (sub-)daily time scales. *Geophys. Res.*
 348 *Lett.*, **39** (12), doi:10.1029/2012GL052261.

349 Rex, D. F., 1950: Blocking action in the middle troposphere and its effect upon regional climate I:
 350 An aerological study of blocking action. *Tellus*, **2** (3), 196–211, doi:10.1111/j.2153-3490.1950.
 351 tb00331.x.

- Scherrer, S. C., M. Croci-Maspoli, C. Schwierz, and C. Appenzeller, 2006: Two-dimensional indices of atmospheric blocking and their statistical relationship with winter climate patterns in the Euro-Atlantic region. *Int. J. Climatol.*, **26** (2), 233–249, doi:10.1002/joc.1250.
- Sillmann, J., M. Croci-Maspoli, M. Kallache, and R. W. Katz, 2011: Extreme cold winter temperatures in Europe under the influence of North Atlantic atmospheric blocking. *J. Climate*, **24**, 5899–5913, doi:10.1175/2011JCLI4075.1.
- Stefanon, M., F. D’Andrea, and P. Drobinski, 2012: Heatwave classification over Europe and the Mediterranean region. *Environ. Res. Lett.*, **7** (1), doi:10.1088/1748-9326/7/1/014023.
- Tibaldi, S., and F. Molteni, 1990: On the operational predictability of blocking. *Tellus A*, **42** (3), 343–365, doi:10.1034/j.1600-0870.1990.t01-2-00003.x.
- Trigo, R. M., I. F. Trigo, C. C. DaCamara, and T. J. Osborn, 2004: Climate impact of the European winter blocking episodes from the NCEP/NCAR Reanalyses. *Climate Dyn.*, **23** (1), 17–28, doi:10.1007/s00382-004-0410-4.
- Whan, K., F. Zwiers, and J. Sillmann, 2016: The Influence of Atmospheric Blocking on Extreme Winter Minimum Temperatures in North America. *J. Climate*, **29** (12), 4361–4381, doi:10.1175/JCLI-D-15-0493.1.
- Woollings, T., 2010: Dynamical influences on European climate: an uncertain future. *Phil. Trans. R. Soc. A*, **368** (1924), 3733–3756, doi:10.1098/rsta.2010.0040.
- Xoplaki, E., J. F. González-Rouco, J. Luterbacher, and H. Wanner, 2003: Mediterranean summer air temperature variability and its connection to the large-scale atmospheric circulation and SSTs. *Climate Dyn.*, **20**, 723–739, doi:10.1007/s00382-003-0304-x.

373 Zwiers, F. W., X. Zhang, and Y. Feng, 2011: Anthropogenic influence on long return pe-
374 riod daily temperature extremes at regional scales. *J. Climate*, **24** (3), 881–892, doi:10.1175/
375 2010JCLI3908.1.

376
377
378
379
380
381
382
383
384
385

LIST OF TABLES

Table 1. Overview on statistics of cold spell days (CSDs) and warm spell days (WSDs). Left columns: Period name and number of total days per (top) season and (bottom) month. Middle columns: (left) number of blocked days (percentage of total days), (middle) number of CSDs (percentage of total days), (right) number of WSDs (percentage of total days). Right columns: (left) number of blocked CSDs (percentage of blocked days / CSDs) and (right) number of blocked WSDs (percentage of blocked days / WSDs). Entries with the number of blocked CSDs/WSDs above (below) the 95th (5th) percentile are marked bold (*italics*). 20

Period	Days	Blocked days	CSDs	WSDs	Blocked CSDs	Blocked WSDs
MAM	3312	1363 (41.15 %)	299 (9.03 %)	519 (15.67 %)	139 (10.20 % / 46.49 %)	280 (20.54 % / 53.95 %)
JJA	3312	961 (29.02 %)	81 (2.45 %)	565 (17.06 %)	<i>11 (1.14 % / 13.58 %)</i>	301 (31.32 % / 53.27 %)
SON	3276	1025 (31.29 %)	308 (9.40 %)	421 (12.85 %)	116 (11.32 % / 37.66 %)	138 (13.46 % / 32.78 %)
DJF	3240	1176 (36.30 %)	554 (17.10 %)	361 (11.14 %)	297 (25.26 % / 53.61 %)	<i>102 (8.67 % / 28.25 %)</i>
Feb	1008	423 (41.96 %)	157 (15.58 %)	103 (10.22 %)	93 (21.99 % / 59.24 %)	<i>24 (5.67 % / 23.30 %)</i>
Mar	1116	395 (35.39 %)	135 (12.10 %)	105 (9.41 %)	61 (15.44 % / 45.19 %)	46 (11.65 % / 43.81 %)
Apr	1080	449 (41.57 %)	80 (7.41 %)	183 (16.94 %)	27 (6.01 % / 33.75 %)	99 (22.05 % / 54.10 %)
May	1116	519 (46.51 %)	84 (7.53 %)	231 (20.70 %)	51 (9.83 % / 60.71 %)	135 (26.01 % / 58.44 %)
Jun	1080	393 (36.39 %)	30 (2.78 %)	181 (16.76 %)	<i>4 (1.02 % / 13.33 %)</i>	111 (28.24 % / 61.33 %)

TABLE 1. Overview on statistics of cold spell days (CSDs) and warm spell days (WSDs). Left columns: Period name and number of total days per (top) season and (bottom) month. Middle columns: (left) number of blocked days (percentage of total days), (middle) number of CSDs (percentage of total days), (right) number of WSDs (percentage of total days). Right columns: (left) number of blocked CSDs (percentage of blocked days / CSDs) and (right) number of blocked WSDs (percentage of blocked days / WSDs). Entries with the number of blocked CSDs/WSDs above (below) the 95th (5th) percentile are marked bold (italics).

LIST OF FIGURES

Fig. 1.	Time evolution of blocking, (a) cold spell days (CSDs), and (b) warm spell days (WSDs) in European spring based on de-trended data. The main panels show blocked days in gray, cold/warm spell days in blue/red, blocked cold/warm spell days in dark blue/red, and blocking within 5 days before a cold/warm spell day in turquoise/orange. The right panels show percentages for each day during spring based on 36 years from 1979 to 2014. The seasonal mean time series are shown for (c) CSDs and (d) WSDs where the trend was removed (top) and not removed (bottom) from the underlying temperature time series.	22
Fig. 2.	Blocking frequency per grid point (shading) coinciding with cold spell days (CSDs) in the European region (gray box). Values that are statistically significantly larger than the number of blocks from random days (above 95th percentile) are marked with a plus sign and values that are statistically significantly lower (below 5th percentile) are marked with a times sign, respectively. (a) Spring (MAM) and (b-f) February to June frequencies. The climatological blocking frequency is indicated by black contour lines.	23
Fig. 3.	As Fig. 2, but for blocking frequency per grid point coinciding with warm spell days (WSDs).	24
Fig. 4.	Number of (a) cold spell days (CSDs) and (b) warm spell days (WSDs) per grid point in the European region over 36 springs from 1979 to 2014. Fraction of (c) CSDs and (d) WSDs per grid point during blocked days. Grid points where the fraction is above (below) the mean value of randomly drawn days are shown in orange (blue) shading. Grid points where the fraction is statistically significantly higher (>95th percentile) or lower (<5th percentile) than the random sample are marked with a dot.	25
Fig. 5.	Blocking frequency per grid point (shading) coinciding with (a,c) cold spell days (CSDs) and (b,d) warm spell days (WSDs) that occur over northern (top) and southern (bottom) Europe. The split into north/south is made at 50°N as indicated by the gray boxes. Values that are statistically significantly larger than the number of blocks from random days (above 95th percentile) are marked with a plus sign and values that are statistically significantly lower (below 5th percentile) are marked with a times sign, respectively. The climatological blocking frequency is indicated by black contour lines.	26

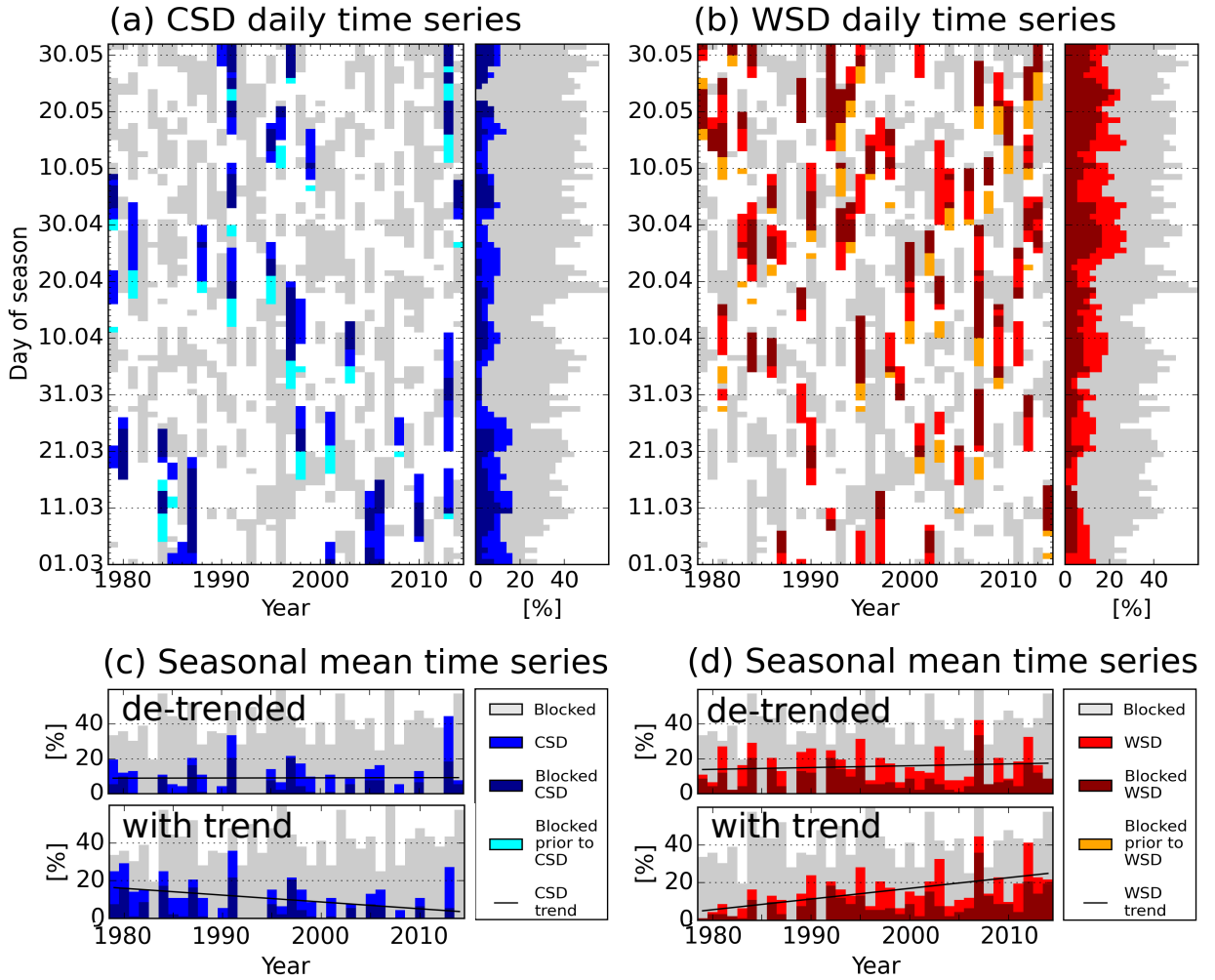


FIG. 1. Time evolution of blocking, (a) cold spell days (CSDs), and (b) warm spell days (WSDs) in European spring based on de-trended data. The main panels show blocked days in gray, cold/warm spell days in blue/red, blocked cold/warm spell days in dark blue/red, and blocking within 5 days before a cold/warm spell day in turquoise/orange. The right panels show percentages for each day during spring based on 36 years from 1979 to 2014. The seasonal mean time series are shown for (c) CSDs and (d) WSDs where the trend was removed (top) and not removed (bottom) from the underlying temperature time series.

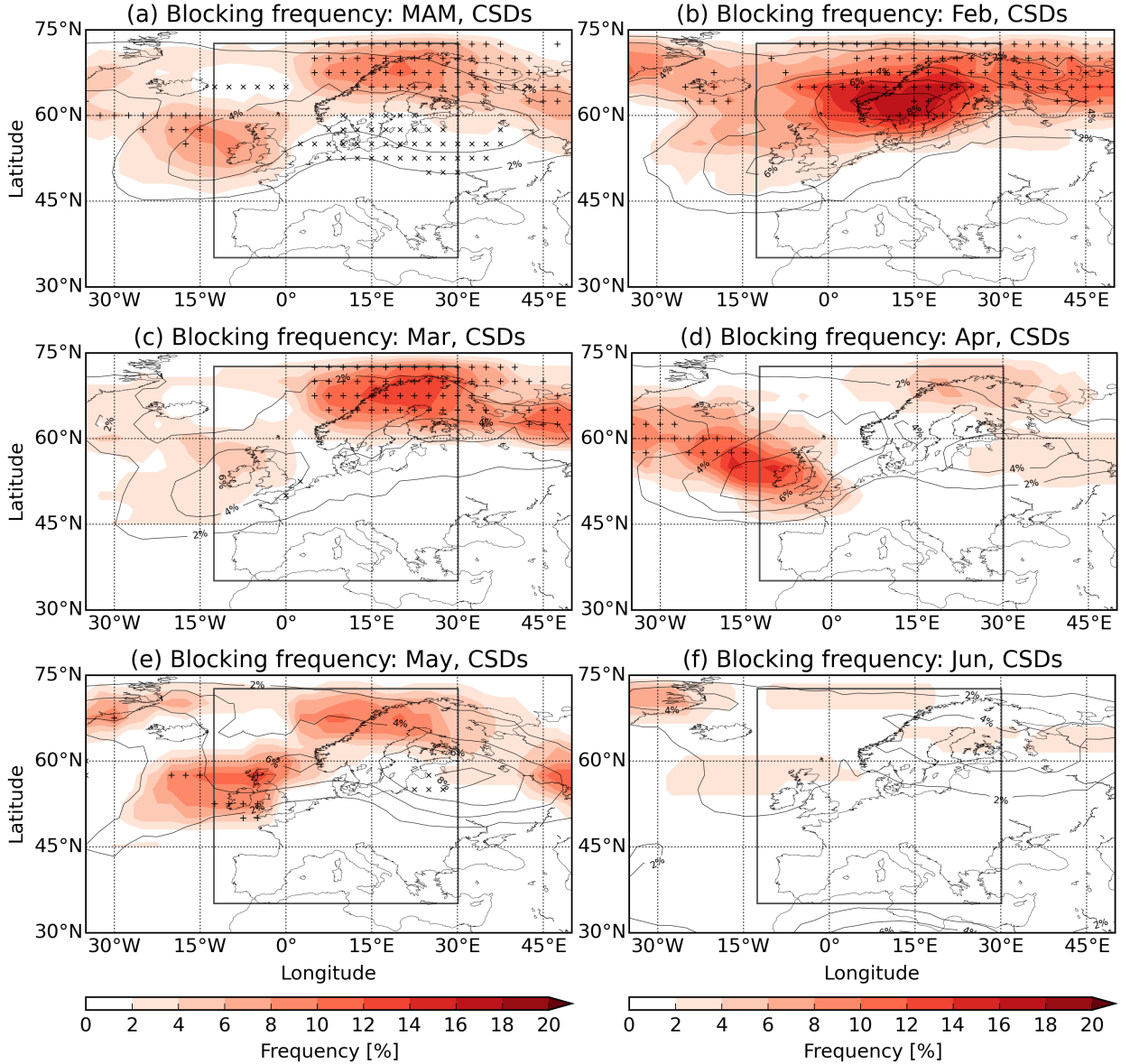


FIG. 2. Blocking frequency per grid point (shading) coinciding with cold spell days (CSDs) in the European region (gray box). Values that are statistically significantly larger than the number of blocks from random days (above 95th percentile) are marked with a plus sign and values that are statistically significantly lower (below 5th percentile) are marked with a times sign, respectively. (a) Spring (MAM) and (b-f) February to June frequencies. The climatological blocking frequency is indicated by black contour lines.

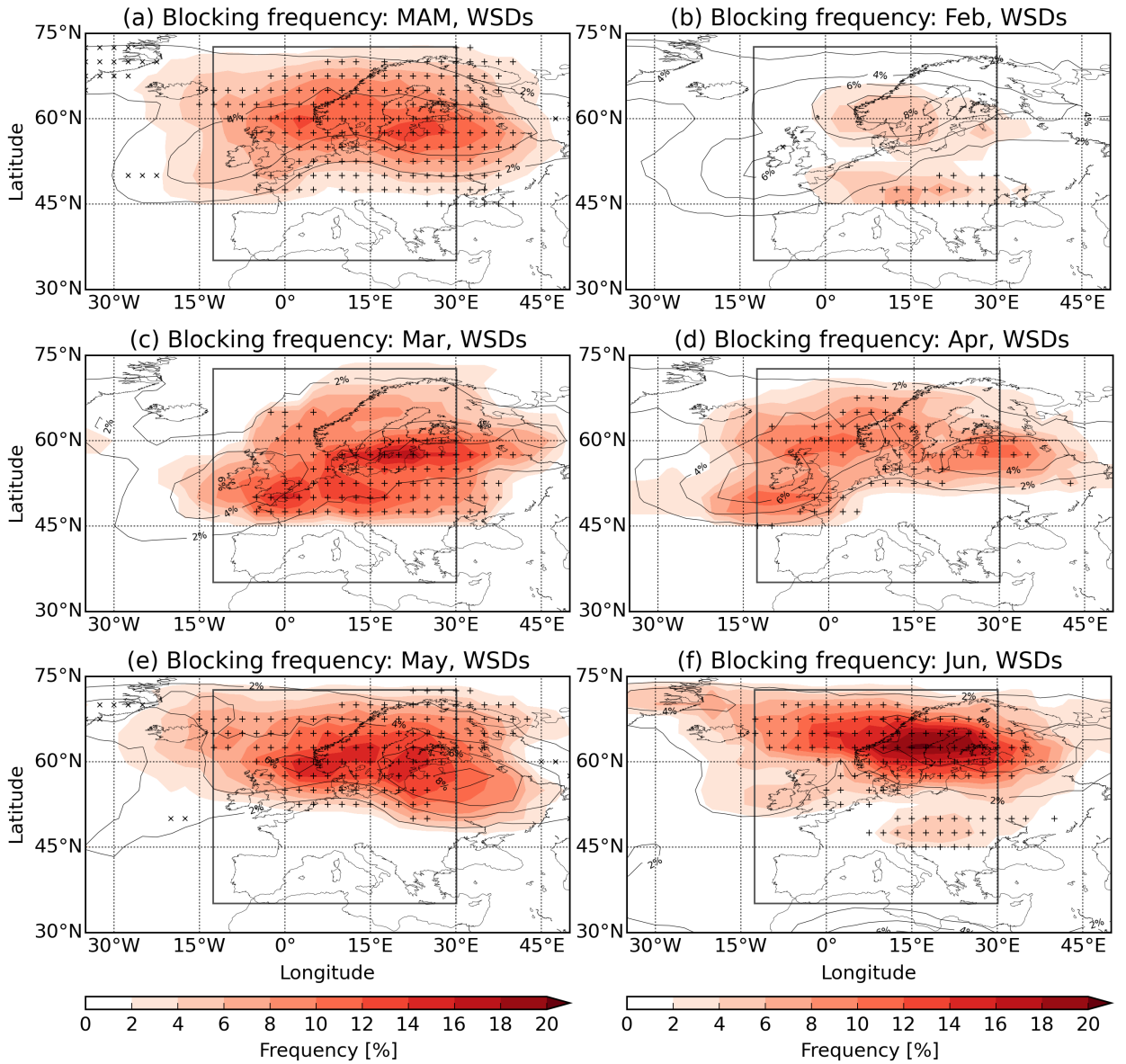


FIG. 3. As Fig. 2, but for blocking frequency per grid point coinciding with warm spell days (WSDs).

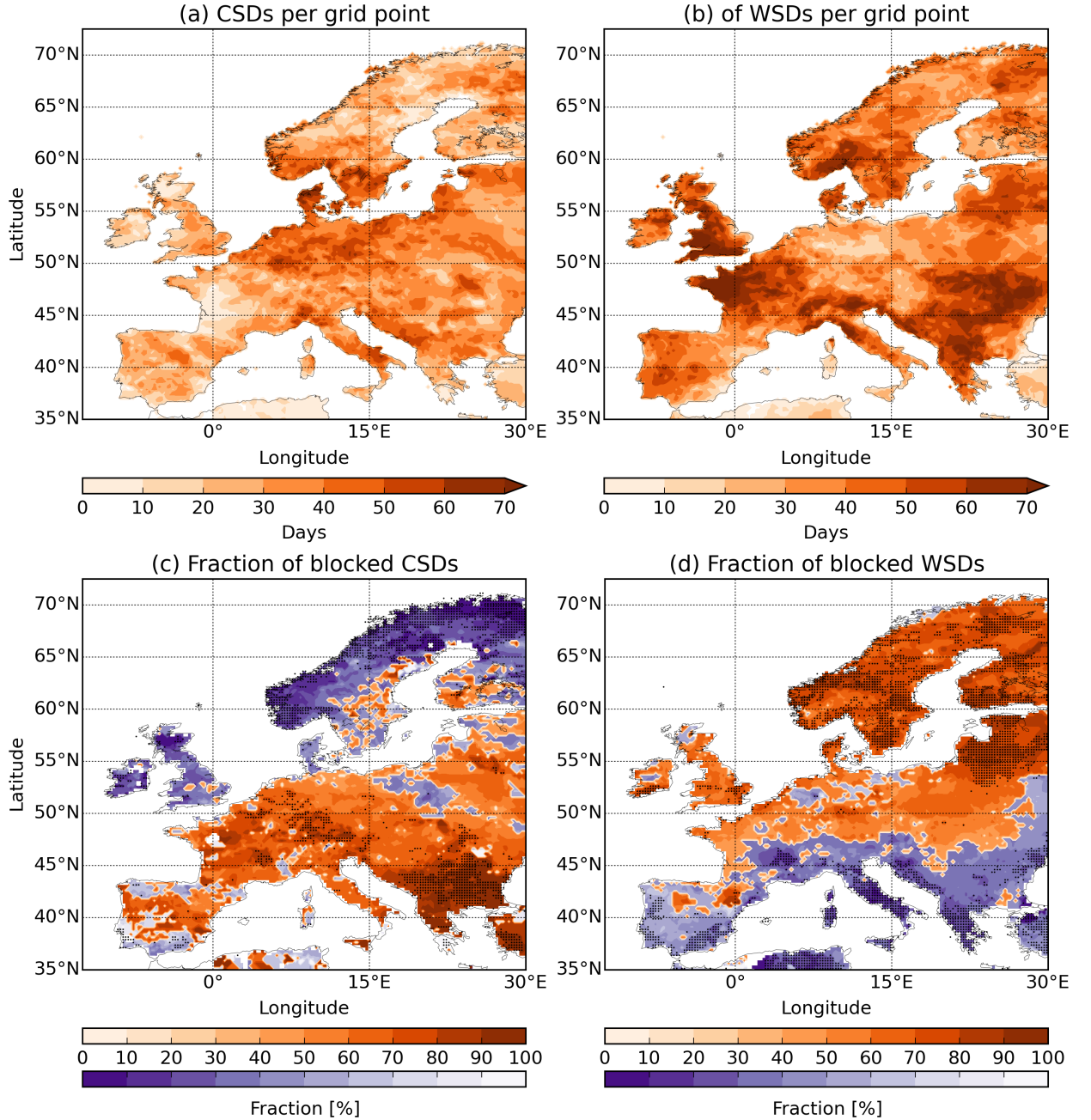


FIG. 4. Number of (a) cold spell days (CSDs) and (b) warm spell days (WSDs) per grid point in the European region over 36 springs from 1979 to 2014. Fraction of (c) CSDs and (d) WSDs per grid point during blocked days. Grid points where the fraction is above (below) the mean value of randomly drawn days are shown in orange (blue) shading. Grid points where the fraction is statistically significantly higher (>95th percentile) or lower (<5th percentile) than the random sample are marked with a dot.

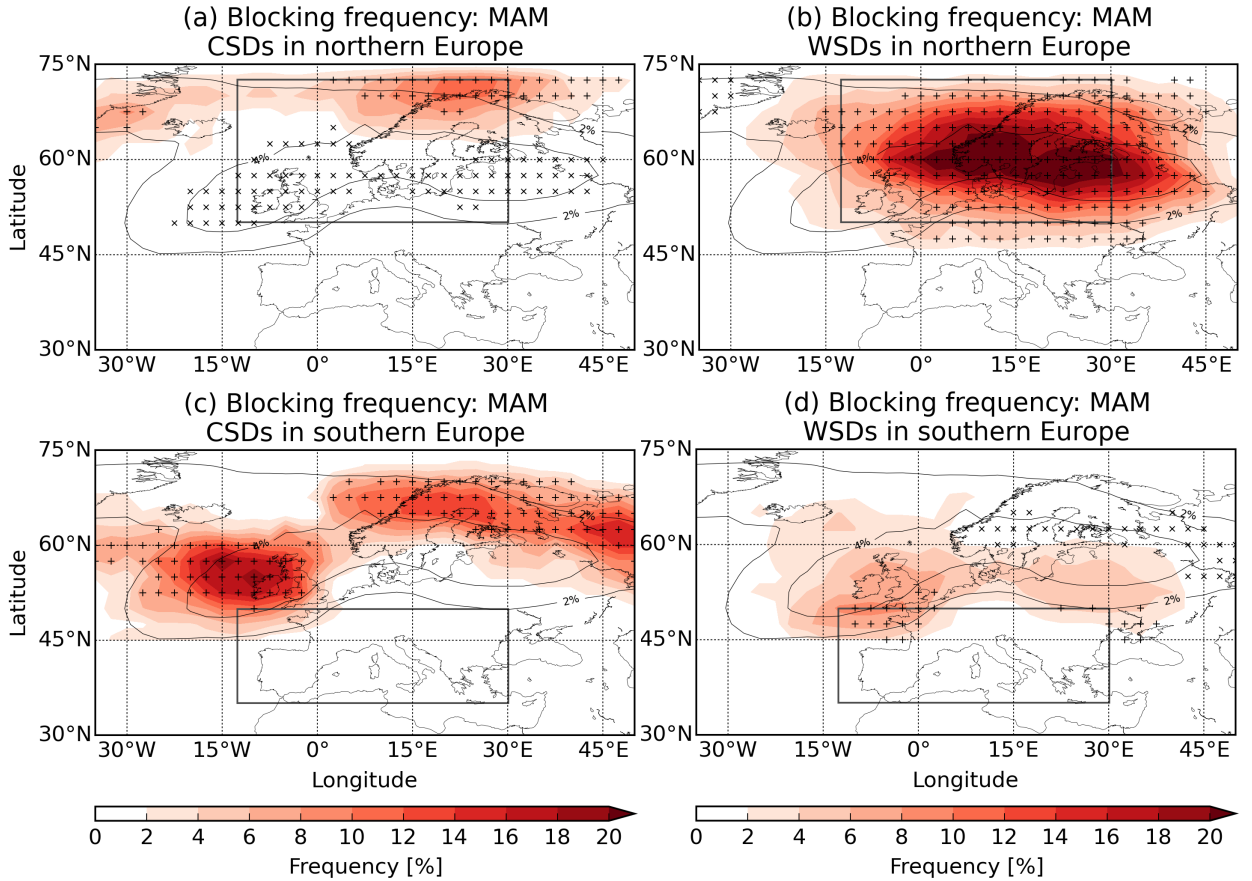


FIG. 5. Blocking frequency per grid point (shading) coinciding with (a,c) cold spell days (CSDs) and (b,d) warm spell days (WSDs) that occur over northern (top) and southern (bottom) Europe. The split into north/south is made at 50°N as indicated by the gray boxes. Values that are statistically significantly larger than the number of blocks from random days (above 95th percentile) are marked with a plus sign and values that are statistically significantly lower (below 5th percentile) are marked with a times sign, respectively. The climatological blocking frequency is indicated by black contour lines.